ARMA/USRMS 05-819

Dynamically Modelling Rock Failure in Percussion Drilling

Gang Han, Mike Bruno
Terralog Technologies USA, Inc., Arcadia, CA, USA
Maurice B. Dusseault
University of Waterloo, Waterloo, ON, Canada

This paper was prepared for presentation at Alaska Rocks 2005, The 40th U.S. Symposium on Rock Mechanics (USRMS): Rock Mechanics for Energy, Mineral and Infrastructure Development in the Northern Regions, held in Anchorage, Alaska, June 25-29, 2005.

ABSTRACT: Percussion drilling attracts the oil and gas industries for its potential to provide faster rate of penetration (ROP) than traditional rotary drilling, especially in hard formations. However, frequent mechanical failures, poor understanding and therefore control of drilling operations have limited its applications in the field. The objective of this research is to advance the fundamental understandings of the physical mechanisms involved in percussion drilling, thereby facilitating more efficient and lower cost drilling and exploration of hard-rock reservoirs. A geomechanical model is presented in this paper to simulate the percussion drilling process. The numerical simulation for rock failure is based on a Mohr-Coulomb model with strain-softening behavior, Rayleigh damping to dissipate excessive oscillation energy, and a fatigue/damage algorithm to update rock properties due to cyclic loading. Important mechanisms for rock failure during percussion drilling, such as aggressive tensile failure due to wave reflection at the rock impact surface, compressive failure due to high axial loading stress, and rock fatigue due to cyclic loading, are captured in the simulation. The insights gained from this study improve the understanding of percussion drilling, and may facilitate development of a simulation tool to better characterize this promising technology.

1. INTRODUCTION

Percussion drilling has long been recognized to have the potential of drilling faster than conventional rotary drill, especially in some hard formations such as granite, sandstone, limestone, dolomite, etc. [1-5]. For example, in Western Canada air hammer methods have expedited well drilling processes by as much as 23 days in one case, compared to normal mud rotary drilling [4]. With the same Weight on Bit (WOB) and Rotation per Minute (RPM), it has been demonstrated that percussive-rotary method could be 7.3 times faster than the conventional rotary method [5].

Other attractions of percussion drilling include lower requirement for WOB, less contact time between bit and rock, longer bit life, less hole deviation, and the generation of larger cuttings [6]. Some additional applications of percussion drilling have been proposed recently, such as using hammer impacts as steady seismic signals to estimate rock properties [7], or as a steerable drilling device to provide down-hole rotation [8], or sources for down-hole electricity generation, etc.

Despite a potential for improved performance with percussion drilling, the oil and gas industries have not shown much enthusiasm in applying this technology in the field. With challenges to drill into deeper and harder formations, air hammers are limited by penetration depth while mud hammers are still in the stage of pre-field development. Unfortunately, there are no hammer performance data for directional wells, slim hole drilling, or coiled tubing drilling. Inconsistent overall results, risks in operation (e.g. mechanical failure), and economic uncertainties are the three main negative factors limiting hammer acceptance and development. Simply increasing impact energy can cause cutters chipped, severe drill string and rig structure vibrations, and even borehole collapse.

Wide acceptance of percussion drilling may not occur until fundamental understanding of the physical mechanisms involved in percussion drilling is more clearly developed. There are some developments recently (e.g. reference [6]), and in this research, we report on three-dimensional dynamic modelling of rock stress, deformation and failure under repetitive loading patterns.

2. HOW PERCUSSION DRILLING WORKS

In conventional rotary drilling, as shown in Fig. 1, WOB first forces the drill bit cutters penetrate into the rock in the direction normal to the bit movement. Then, the cutters shear off a conchoidal chip of the penetrated rock as the bit rotates. There are two requirements for a rotary drill to advance through the rock: first WOB must be high enough to press the cutters into rock; and second, the cutters must generate and localize enough shear stress to break the rock, an issue related to rotation speed and cutter properties.

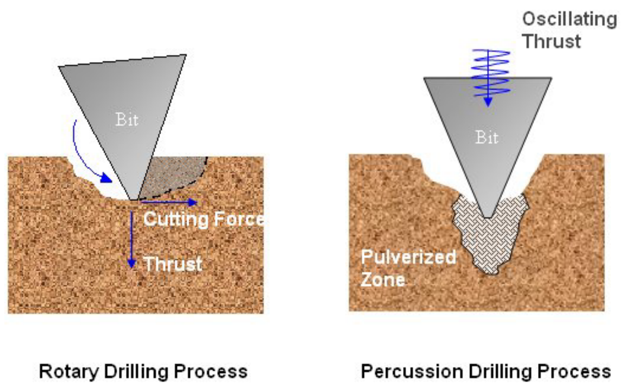

Fig. 1. Illustration of rock defragmentation in rotary and percussion drilling

With high impact speed and short contact time, based on the Law of Conservation of Momentum, the drill bit in percussion drilling can produce much higher impact force along the direction of bit movement (Fig. 1). When the force exceeds rock compressive strength, it crushes the rock below the bit and creates fractures forming a narrow wedge along the outer boundaries of the bit inserts. The cratered zone may extend to a depth several times greater than the actual depth of bit penetration [9].

A condition for percussion drilling is accelerating the drill bit to an impact speed high enough to overcome rock strength. Another consideration is cuttings removal and transport. Failed rock needs to be removed as quickly as possible so that a fresh rock surface is available for the next impact. Otherwise most of the percussive energy will dissipate by rock fragment attrition instead of contributing to penetration. For air hammer, both acceleration and the efficiency of cuttings removal become insufficient as depth becomes large. Mud hammers therefore have greater potential for drilling into deeper and harder formations.

3. MODELLING EFFORTS

To investigate the rock deformation and failure during percussion drilling, a 3D numerical model was developed with aid of a commercial stress code [13]. The simulation includes a Mohr-Coulomb type strain-softening model, Reyleigh damping to dissipate excessive oscillation energy, criteria to describe when and how rock experiences failure, and a fatigue/damage algorithm to update rock properties alteration (e.g. cohesive strength and tensile strength changes) as the result of cyclic loading. Disintegrated rock is assumed to be removed immediately after failure.

3.1. 3D Model configuration

Figure 3 presents the model configuration. It is a square cross-section area with a side length of 1.5 m and a total height of 3 m. The vertical borehole has a total depth of 0.5 m and a diameter of 0.178 m. The applied boundary conditions are a constant lateral confinement of 12.5 MPa, an overburden stress of 15 MPa and a fixed displacement boundary condition at the bottom surface. The hammer impacts the rock at the borehole bottom with a maximum speed of 5m/s and it lasts 3×10^{-4}sec for each of 5 impacts. Table 1 lists the inputs used in the 3D configuration.

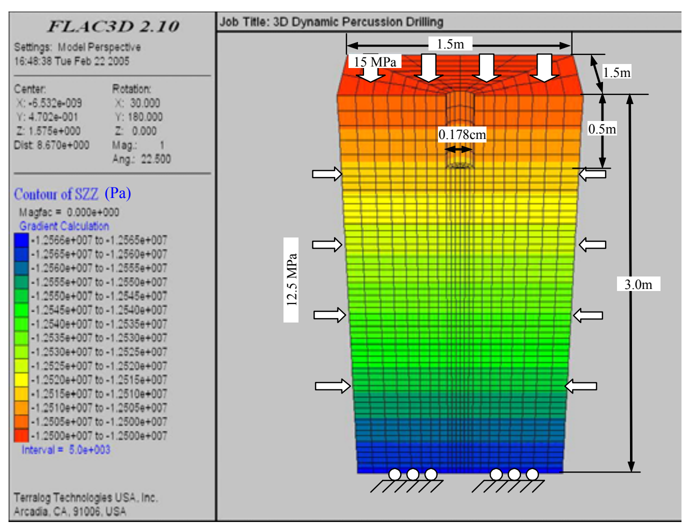

Fig. 3. Simulation configurations in 3D percussion drilling.

Table 1. Inputs for 3D simulation of percussion drilling

Model Size(X×Y×Z)	1.5m×1.5m×3.0m
Wellbore diameter	0.178 (m)
Confining stress	12.5 (MPa)
Overburden pressure	15 (MPa)
Peak impact velocity	6 (m/s)
Number of impacts	5
Cycle period	6×10^{-4}(s)

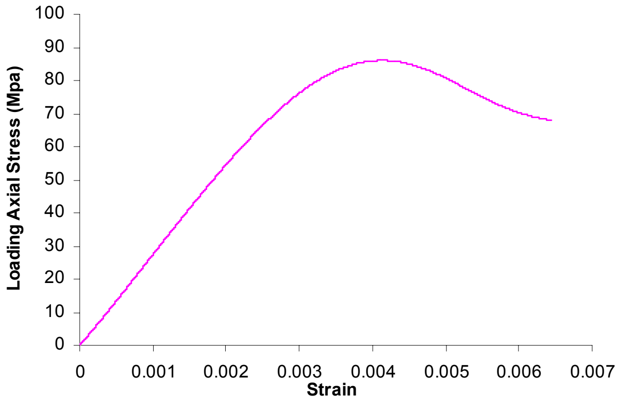

Fig. 2. Stress-strain curve for a hard rock tested.

3.2. Material model

The material is a hard rock with strain-softening behavior. Its peak strength is defined by Mohr-Coulomb criteria:

$$\sigma_1 - \frac{1+\sin(\varphi)}{1-\sin(\varphi)}\sigma_3 - \frac{2\cos(\varphi)c_o}{1-\sin(\varphi)} = 0 \qquad (1)$$

where σ_1 and σ_3 are maximum and minimum principal compressive stresses, c_o is cohesive strength, and φ is the friction angle. Rock properties are summarized in Table 2. The relationship between strength and strain is specified in Table 3. The rock behavior upon loading, i.e. stress-strain curve, is plotted in Fig. 2 for σ_3 = 12.5 MPa.

Table 2. Rock properties applied in the model

Rock Density	2.25 (g/cm^3)
Bulk Modulus	12 (GPa)
Shear Modulus	7.25 (GPa)
Compressive Strength	10.24 (MPa)
Friction Angle	30 (degrees)
Tensile Strength	1.2 (MPa)
Fatigue Coefficient, a	0.9987
Fatigue Coefficient, b	-0.0313

Table 3. Softening table for strength and friction angle

Plastic strain	0	4×10^{-4}	6×10^{-4}	1×10^{-3}	2×10^{-3}
Cohesion (MPa)	10.24	9.86	9.52	8.52	8.06
Friction angle	30	29	28.5	28	26

3.3. Failure models

Before further discussion of the failure model, it is necessary to clarify two terms that are often misused: rock yield and failure. Yield refers to a process of accumulation of shear bands or microfissures developed as rock starts to gradually lose its ability to support load, whereas failure means collapse and total loss of strength.

Three rock failure criteria are applied. Failure can occur due to 1) excessive compressive strain; 2) excessive tensile stress; and 3) excessive plastic shear strain. The rock is assumed to completely lose its ability to support further loading after failure.

A critical compressive strain is proposed to describe when rock fails due to excessive compressional strain in loading direction:

$$\varepsilon_{zz} > \bar{\varepsilon}_z \qquad (2)$$

where ε_{zz} is calculated compressional strain in loading direction, and $\bar{\varepsilon}_z$ is the critical strain value determined from lab testing. In the model $\bar{\varepsilon}_z = 0.006$ is used.

For plastic shear strain failure,

$$\varepsilon^{ps} > \bar{\varepsilon}_{ps} \qquad (3)$$

where εps is calculated plastic shear strain and $\bar{\varepsilon}_{ps}$ is determined from lab testing.

For tensile failure,

$$\sigma_1 > \sigma_T \qquad (4)$$

where σ_1 is the maximum principal stress and σ_T is the critical tensile strength determined from lab testing or suitable correlations. This type of failure most likely occurs during bit retreat when the compressive stress wave is reflected in tension, a significant case if there is not enough Bottom Hole Pressure (BHP), such as in drilling with an air hammer. This case is investigated in this study.

3.4. Fatigue/damage model

Rock may become weakened after cyclic loadings even if the loading stress is substantially below its peak strength defined in Eq. (1). This has been studied in petroleum geomechanics as "rock fatigue" (e.g. [11, 12]), while rock damage may result from both strain-weakening process and fatigue. To simulate fatigue in percussion drilling, an algorithm is applied to update both rock cohesive strength and tensile strength at the end of each loading-unloading cycle, providing that the loading stress reaches 75% of rock peak strength [12],

$$y = ax^b \qquad (5)$$

where x is number of cycles, and y is the ratio of rock peak strength to initial strength. Values of two coefficients, listed in Table 1, are determined from lab experiments or suitable correlations.

3.5. *Damping*

When a stress wave passes through rock, part of its energy is lost as a result of internal friction. Rayleigh damping is applied in this research, and the two parameters in the algorithm are a critical wave frequency related to rock mass and modulus, and a damping ratio describing how much range of the frequency can be efficiently damped [13].

4. SIMULATIONS AND DISCUSSIONS

4.1. *Model inputs and simulation outline*

In addition to parameters listed in Table 1 and 2, a stress wave input as a dynamic loading condition is also needed. The time-dependent impact velocity on the first rock element is defined as

$$v = v_{\max} \sin\left(\frac{2\pi}{T} t\right) \qquad (6)$$

where v_{max} is the maximum impact velocity and T is the cycle period. Their values are listed in Table 1.

Upon receiving the impact, rock will deform elastically first and then elastoplastically after the stress exceeds rock strength. As soon as rock failure occurs, as determined by the three failure criteria, failed elements will be removed as cuttings and the remaining impact will continue to load on the next stable element adjacent to the failed ones. After each cycle of impact, rock properties such as cohesive strength and tensile strength will be updated for those unfailed elements.

4.2. *Rock fatigue and damage*

To focus on rock fatigue and damage, we can disable rock failure and removal. Fig. 4 shows how cohesive and tensile strength of the first rock element that hammer impacts (i.e. the element at the borehole bottom). Generally both strengths decrease with number of cycles. There is, however, a sharp drop in cohesive strength after the first impact. This is because the element has experienced strain-weakening during its elastoplastic deformation, which affects rock cohesive strength in a way defined in Table 2.

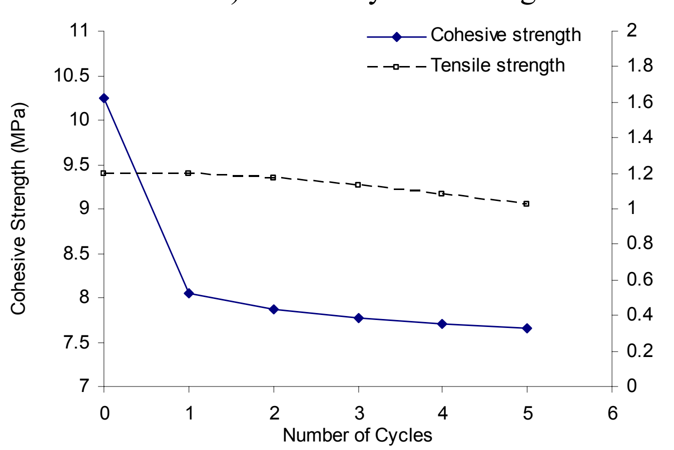

Fig. 4. Rock fatigue and damage with cyclic loading.

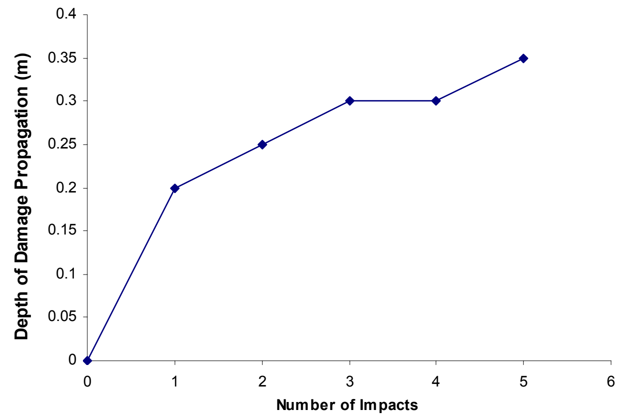

Fig. 5. Rock damage propagation with cyclic loading.

Fig. 5 shows how deep the damage can reach after each loading cycle. The first impact can damage the rock 0.2m deep from the bottom-hole while at the end of 5 cycles of loading, the damage has propagated 0.35m below the impact surface.

4.3. *Effect of damping*

The rock damping effect on stress wave propagation is now explored. Figs 6, 7, 8 demonstrate velocity evolution for the first impacted element under the conditions of large damping (60% of the critical frequency is obsorbed), small damping (20% of the critical frequency is obsorbed), and no damping, respectively. After being applied to rock surface for 3×10^{-4}sec in a sine form, the impact is removed while hammer retreats.

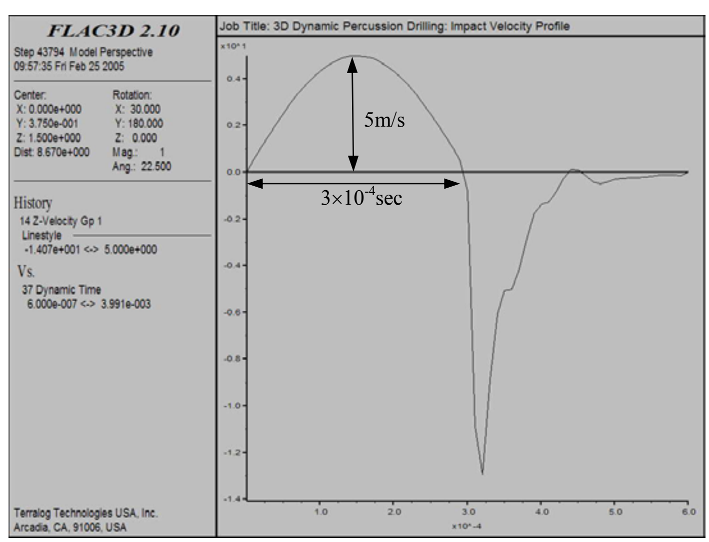

Fig. 6. Rock vertical velocity at the impact surface (large damping, 60%).

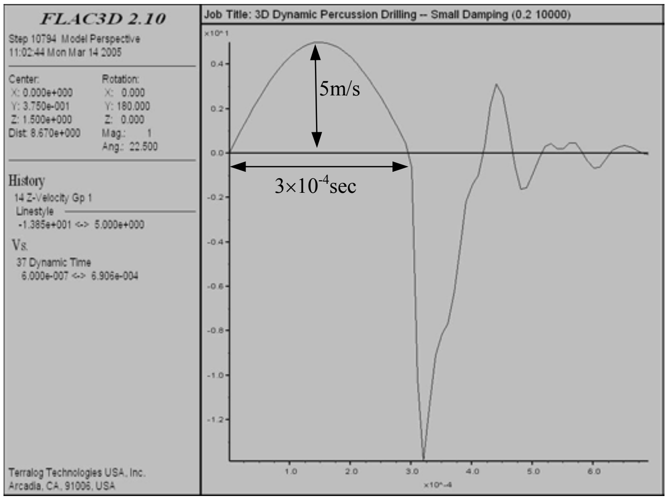

Fig. 7. Rock vertical velocity at the impact surface (small damping, 20%).

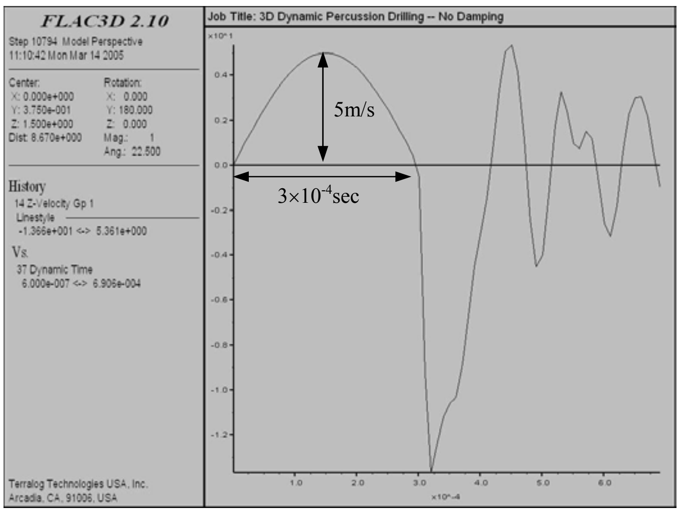

Fig. 8. Rock vertical velocity at the impact surface (no damping).

With more vibration energy being absorbed, the magnitude of reflected waves becomes smaller, and the oscillation diminishes more quickly. Damping parameters must therefore be selected carefully so that simulation results can closely replicate rock behavior.

4.4. *Rock failure and bit advancement*

After implementing rock failure model and selecting appropriate damping features, the bit advance with 5 cycles of hammer impacts is simulated and plotted (Fig. 9). Each jump of the curve indicates a removal of a failed rock element.

The velocity profile of elements close to the impact surface is plotted in Fig. 10. Each curve represents one rock element close to the impact. The

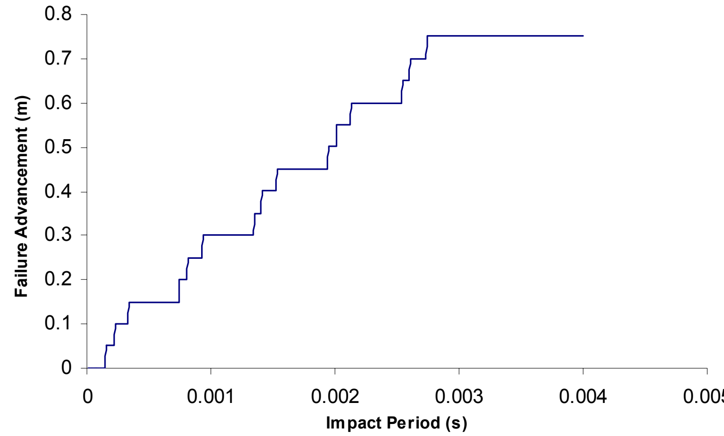

Fig. 9. Bit advancement during percussion drilling.

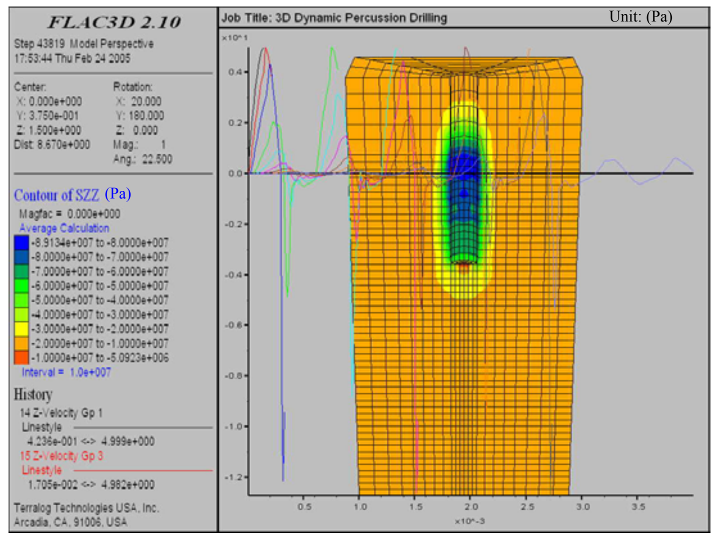

Fig. 10. Rock stress and velocity profiles after 5 impacts in percussion drilling.

discontinuity of some curves is because the failed elements that the curves correspond to are removed. The sudden jump of the velocity profiles accounts for the effect that after an element has failed, the hammer velocity is immediately transferred to the next adjacent element since cuttings removal from the failed surface is assumed to be instantaneous.

Along with profiles of rock stress and deformation and history of bit advancement, another output is a file documenting rock failure history, as shown in Fig. 11. Most of the failed rock elements are due to compression during hammer-rock impact. However, there are quite a few elements have experienced failure in tension during hammer retreat and wave reflection.

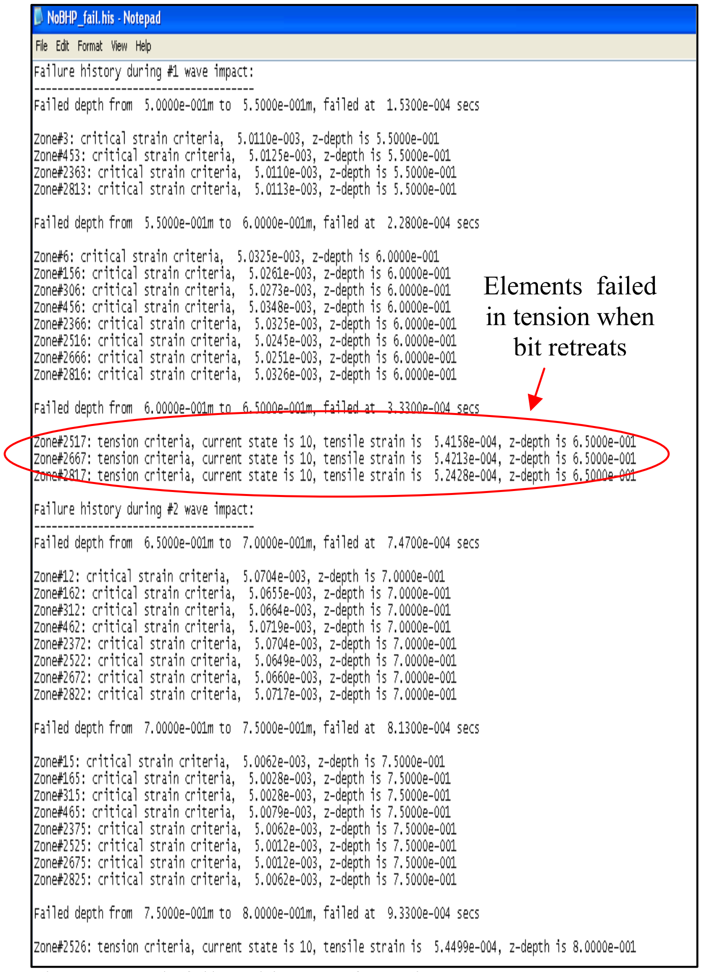

Fig. 11. Rock failure history after 2 impacts.

4.5. Limitations and further development

While significant efforts have been made to address main critical issues in percussion drilling process, some simplifications have also been taken:

- The model does not account for bit rotation, which results in efficient indexing. As long as some elements are failed, the layer at the same depth as the failed elements is to be removed under the impact surface; this leads to overestimation of results, such as ROP;
- The model does not account for fluid flow, which takes time to clean the hole bottom. The removal of failed elements is assumed to be instantaneous, which is another contributor to overestimation of ROP. This, however, can be relaxed by extending period of the percussion cycle;
- The model does not account for shape and size of the cutter. The impact forces/velocities are imposed on the first rock layer of the rock-bit contact surface. However, bit shape and size can be considered by the introduction of an impact force/velocity function to portions of the first layer, instead of the whole layer.

Nevertheless, the model developed, to the authors' knowledge, is the first numerical attempt to simulate a true 3D percussion drilling process based on sound physics. It can be used to further investigate and understand rock mechanics aspects of percussion drilling, such as the effect of BHP on the drilling process. It also can be used to select and optimize operating parameters to maximum ROP under specified conditions.

A set of full-scale laboratory hammer tests are now under way. The purpose of the tests is to verify the physics and mechanisms described in the theoretical models, and also to validate the simulation development. The full-scale tests will allow us to better understand the values of the parameters used in the model, and therefore to select more reasonable values for field drilling work.

5. CONCLUSIONS

Despite being an attractive technology for stiff brittle rocks, applications of percussion drilling in the oil and gas industries have been restrained by poor understanding of percussion drilling mechanisms. To model percussion drilling, we used a Mohr-Coulomb type material model with strain-softening behavior, failure models to describe when and how rock fails, a Rayleigh damping feature to dissipate excessive oscillation energy, and a fatigue/damage algorithm to update rock properties due to cyclic loading. The hammer effect was simulated with a sine wave of impact velocity. In this way, dynamic modeling of rock failure under a repetitive loading pattern was achieved.

The numerical simulations generate three outputs, a plot of failure advancement, a history of rock failure, and a history of rock fatigue/damage. The rock failure history describes when and how many rock elements have failed and what type of failure they have experienced, while the rock fatigue/damage history demonstrates how rock fatigue and damage develop and evolve as a result of repeated impacts.

These studies have already advanced fundamental understanding of the physical mechanisms involved in percussion drilling. After calibrations with a set of full-scale hammer tests, the simulation tool may facilitate the study of more efficient and lower cost drilling methods for penetration of hard, brittle rocks that are drilled in the search for oil and gas resources. Of course, percussion drilling is used in other industries such as mining and rock excavation.

6. ACKNOWLEDGEMENTS

The authors thank Department of Energy for partially funding this research under contract DE-FC26-03NT41999. Dr. Luis Dorfmann and Mr. Khang Lao have provided valuable support to this project. Technical discussions with Dr. Sidney Green, Mr. Arnis Judzis, and Mr. Alan Black at TerraTek, and Mr. Shantanu Swadi at Smith Bits, Mr. David Pixton at NovaTek, and Prof. Marian Wiercigroch and Joe Emans at the University of Aberdeen are appreciated.

REFERENCES

1. Harpst, W.E. and E.E. Davis. 1949. Rotary percussion drilling, *Oil and Gas Journal*, November, 10.
2. Wanamaker, J.A. 1951. Rotary percussion drilling in west Texas. *World Oil*, September, 182-187.
3. Whiteley, M.C. and W.P. England. 1986. Air drilling operations improved by percussion-bit/hammer-tool tandem. SPE 13429, *SPE Drilling Engineering*, Octomber, 377-382.
4. Pratt, C.A. 1987. Modifications to and experience with percussion air drilling. SPE/lADC 16166, *the SPE/ IADC Drilling Conference*, New Orleans, LA, USA, 15-18 March 1987.
5. Melamed, Y., A. Kiselev, M. Gelfgat, D. Dreesen, and J. Blacic. 2000. Hydraulic hammer drilling technology: developments and capabilities. *Journal of Energy Resources Technology*, 122(1): 1-8.
6. Han, G., M. Bruno, and K. Lao. 2005. Percussion drilling in oil industry: review and rock failure modelling, AADE-05-NTCE-59, *the AADE 2005 National Technical Conference and Exhibition*. Houston, TX, 5-7 April 2005.
7. Minear, J.W., D.R. Heysse and P.M. Boonen. 1996. Initial results from an acoustic Logging-While-Drilling tool. SPE 36543.
8. Bui, H., J. Meyers and S. Swadi. 1995. Steerable percussion air drilling system. DOE contractor review meeting. Baton Rouge, USA, April.
9. Faihust, C., and W.D. Lacabanne. 1956. Some principles and developments in hard rock drilling techniques. *Proc. 6th Ann. Drilling and Blasting Symposium*, Minnesota Uni., 15-25.
10. Itasca Consulting Group, Inc., 2002. *FLAC3D: theory and background*. Minneapolis, Minnesota, USA.
11. Cheng, H. and M.B. Dusseault, 2002. Continuum damage theories and petroleum geomechanics, SPE78198, *the SPE/ISRM Rock Mechanics Conference*, Irving, TX, USA. 20-23 October 2002.
12. Ewy, R.T., C.A. Bovberg, G. Chen, R. Jansson, and G. Pepin, 2004. Fatigue testing of hollow cylinders and application to injection well cycling. ARMA/NARMS 04-464, *the 6th North America Rock Mechanics Symposium.* 5-9 June 2004.
13. Itasca Consulting Group, Inc., 2002. *FLAC3D: optional features*. Minneapolis, Minnesota, USA.